Published in final edited form as:
Arch Pharm Res. 2014 December ; 37(12): 1607–1616. doi:10.1007/s12272-013-0257-5.

The osmotic stress response of split influenza vaccine particles in an acidic environment

Hyo-Jick Choi,
Nanotechnology Accelerator and Department of Chemical and Materials Engineering, National Institute for Nanotechnology, University of Alberta, Edmonton, AB T6G 2M9, Canada

Min-Chul Kim,
Animal and Plant Quarantine Agency, Anyang, Gyeonggi-do 430-757, Korea

Sang-Moo Kang, and
Center for Inflammation, Immunity and Infection and Department of Biology, Georgia State University, Atlanta, GA 30303, USA

Carlo D. Montemagno
Nanotechnology Accelerator and Department of Chemical and Materials Engineering, National Institute for Nanotechnology, University of Alberta, Edmonton, AB T6G 2M9, Canada

Hyo-Jick Choi: hyojick@ualberta.ca; Carlo D. Montemagno: montemag@ualberta.ca

Abstract

Oral influenza vaccine provides an efficient means of preventing seasonal and pandemic disease. In this work, the stability of envelope-type split influenza vaccine particles in acidic environments has been investigated. Owing to the fact that hyper-osmotic stress can significantly affect lipid assembly of vaccine, osmotic stress-induced morphological change of split vaccine particles, in conjunction with structural change of antigenic proteins, was investigated by the use of stopped-flow light scattering (SFLS), intrinsic fluorescence, transmission electron microscopy (TEM), and hemagglutination assay. Split vaccine particles were found to exhibit a step-wise morphological change in response to osmotic stress due to double-layered wall structure. The presence of hyper-osmotic stress in acidic medium (0.3 osmolarity, pH 2.0) induced a significant level of membrane perturbation as measured by SFLS and TEM, imposing more damage to antigenic proteins on vaccine envelope than can be caused by pH-induced conformational change at acidic iso-osmotic condition. Further supports were provided by the intrinsic fluorescence and hemagglutinin activity measurements. Thus, hyper-osmotic stress becomes an important factor for determining stability of split vaccine particles in acidic medium. These results are useful in better understanding the destabilizing mechanism of split influenza vaccine particles in gastric environment and in designing oral influenza vaccine formulations.

Correspondence to: Hyo-Jick Choi, hyojick@ualberta.ca; Carlo D. Montemagno, montemag@ualberta.ca.

Conflict of interest The authors declare no conflict of interest.

Electronic supplementary material The online version of this article (doi:10.1007/s12272-013-0257-5) contains supplementary material, which is available to authorized users.

Keywords

Influenza vaccine; Split vaccine particle; Whole inactivated virus vaccine particle; Osmotic stress; Stopped-flow light scattering

Introduction

Influenza viral infection is responsible for causing epidemic and pandemic respiratory disease resulting in high morbidity and mortality (Thompson et al. 2003). Vaccination is the most efficient strategy in impeding the infection, but mutations in antigenic glycoproteins require annual reconfiguration and revaccination to induce the appropriate immune response (Harper et al. 2004). Mass vaccination using intramuscular/intradermal is not sustainable due to the high cost, difficulty of administration, and concerns over safety/waste management. Intranasal immunization has been gaining attention due its ability to induce mucosal and systemic immune responses without transcutaneous injection (Neutra and Kozlowski 2006). However, intranasal influenza vaccine is not administered to the most high-risk populations for infection/mortality (Fiore et al. 2010) and some formulations have been removed from the market due to safety issues (Mutsch et al. 2004; Palese 2006).

As a potential alternative, focus on oral vaccination has increased. Advantages of oral vaccinations include a lack of biohazardous waste, reduced costs (no needles/syringes, no need for highly trained personnel), easier production, and potential self-administration (Giudice and Campbell 2006). However, a major drawback of any oral influenza vaccine is a significant decrease in immunogenicity and protective efficacy as a result of vaccine destabilization in the acidic gastric environment (Lazzell et al. 1984; Farag-Mahmod et al. 1988; Quan et al. 2011). As a result, vaccines must contain a greater amount of antigen, reducing any economic advantages (Farag-Mahmod et al. 1988; Neutra and Kozlowski 2006; Azizi et al. 2010). pH-induced structural change has been concluded to be the cause of decreased immunogenicity (Skehel et al. 1982; Bullough et al. 1994). However, irreversible pH-dependent conformational changes are not likely to be the lone reason for this activity loss. Thus, a mechanistic understanding of the effects of the physiochemical gastric environment on vaccine stability is considered to be an important step toward developing a high efficacy oral influenza vaccine.

Digestion is a complex process that includes chemical degradations, osmotic stress, and biological catabolism (Hunt 1959; Szarka and Camilleri 2009). In a recent study, we investigated destabilization mechanisms of whole inactivated influenza virus (WIV) vaccine under simulated gastric conditions, focusing on the effects of pH, temperature, gastric retention time, osmotic pressure, and dilution on the stability of vaccine (Choi et al. 2013b). It was shown that vaccine particles exhibited a step-wise morphological change, and that vaccine destabilization was associated with the combined effects of low pH-induced degradation of antigens and osmotic stress-induced morphological changes of the vaccine particles. Furthermore, in the same report we demonstrated that hyper-osmotic stress induced irreversible destruction of the virus morphology, significantly enhancing destabilization of WIV vaccine particles in an acidic environment in contrast to hypo- and

iso-osmotic stress. Clearly, the characteristics of the osmotic-response of enveloped vaccine particles have a substantial impact on functional activity of oral vaccines in gastric environment.

In the present study, we used stopped-flow light scattering (SFLS) analysis to investigate the osmotic stress-induced morphological change of inactivated A/PR/8/34 (H1N1) split vaccine particles associated with functional activity in an acidic environment. Microscopic membrane destabilization and morphological change of the vaccine particles were predicted from the correlation between volume and scattered light intensity established for liposomes. A comparative study of osmotic stress-induced swelling/shrinkage behavior of split vaccine particles and WIV vaccine particles was performed after exposure to hypo-, iso-, and hyper-osmotic gradients. Transmission electron microscopy (TEM), intrinsic fluorescence, and hemagglutination activity were measured to determine pH-induced morphological change of vaccine, conformational change of antigens, and functional activity of hemagglutinin (HA).

Materials and methods

Preparation of WIV influenza vaccine

Whole inactivated A/PR/8/34 (H1N1) influenza A virus vaccine was prepared as described elsewhere (Quan et al. 2008). Briefly, A/PR/8/34 virus was grown in chicken's eggs and purified from allantoic fluids of infected eggs by a discontinuous sucrose density gradient centrifugation. The purified virus was inactivated with formalin at a final concentration of 1:4,000 (v/v). Viral inactivation was confirmed by plaque assay with Madin-Darby canine kidney cells and by the absence of the infectious influenza virus after inoculation into embryonated chicken's eggs.

Preparation of split influenza vaccine

Split influenza vaccine was prepared by treatment of WIV vaccine with Triton X-100 (Sigma Aldrich, St. Louis, MO). In brief, 1 ml of WIV was mixed with 9 ml of 10 % Triton X-100 for 2 h, and then dialyzed at 4 °C aginst phosphate-buffered saline. The buffer was replaced three times for 3 h in a 10,000 Da cutoff dialysis cassette (Thermo Scientific, Rockford, IL, USA), followed by overnight dialysis at 4 °C. After dialysis, split vaccine particles were collected and stored at −80 °C.

SFLS analysis

Osmotic swelling/shrinking behavior of influenza vaccine particles was investigated by monitoring time-dependent changes in light scattering intensity after mixing with different concentrations of sucrose solutions in a stopped-flow apparatus (MOS-200/M spectrometer, SFM-20; Bio-Logic USA, Knoxville, TN, USA). SFLS spectra were recorded with the following instrumental conditions: excitation wavelength 546 nm; injection volume 66μl; flow rate 7 ml/s; scan range 8, 80, 400, and 7,200 s; temperature 4 °C. A rate constant (k) was obtained from curve fitting of the spectra with a single exponential equation ($I = a + b \cdot e^{-k \cdot t}$) using Bio-Kine 32 V4.46 software (Bio-Logic USA) (Choi et al. 2013a).

The transmembrane osmotic gradient (Δ) was defined as the difference in osmolarity (osM) between the external and inner medium ($=C_{ex} - C_{in}$, where C_{in} is 0.3 osM) across the viral membrane. To characterize morphology at a very early stage of incubation, 8-s scan SFLS analysis was performed at 4 °C by exposing iso-osmotic vaccine suspension in 300 mM sucrose (pH 7.0) to various concentrations of acidic sucrose solutions (pH 1.7) in an equal volume ratio; i.e., hypo-osmotic (Δ = −0.15, −0.1, −0.075, and −0.05 osM), iso-osmotic (Δ = 0 osM), and hyper-osmotic (Δ = 0.025, 0.05, 0.1, 0.15, and 0.3 osM) gradients. To monitor the step-wise morphological change of influenza vaccine, additional scans were carried out over different incubation periods (80, 400, and 7,200 s) at 4 °C considering long-term morphological change of orally administered vaccine.

Morphological change of influenza vaccine particles

Time-dependent size changes of influenza vaccine particles under various acidic environments were assessed via SFLS plot analysis. The size of the vaccine particles was calculated using the previously reported correlation between the SFLS intensity and the size of phosphatidylcholine-liposomes (Choi et al. 2013b). In this work, liposomes served as a reference for SFLS data interpretation of influenza vaccine particles under the hypothesis of a similar response to osmotic stress. Briefly, osmotic stress corresponding to each SFLS data point at time t (Δ_t) is calculated using an empirical function $I_{rel} = 1 + c \cdot e^{x/\Delta t} + d \cdot e^{y/\Delta t}$, where c, d, x, and y were −0.11653, −2.28333, 0.09645, and 1.61951, respectively, for hypo-osmotic stress and 0.14824, 5.14043, −0.21065, and −3.30994, respectively, for hyper-osmotic stress, to establish the relationship between I_{rel} = and Δ_t. Then, Δ_t is used to determine the vaccine volume change relative to the iso-osmotic volume ($V_{rel} = V/V_{iso}$) using equations: $V_{rel} = 1 - 0.52879 \cdot \Delta_t$ for $\Delta_t \leq 0$, $V_{rel} = 0.79 + 0.21 \cdot (C_{in}/C_{ex})$ for $0 < \Delta_t < 0.46$, and $V_{rel} = 0.07 + 2.03 \cdot (C_{in}/C_{ex})$ for $\Delta_t \geq 0.46$. However, this method resulted in 0.02 lower and 0.015 higher V_{rel} values at $I_{rel} = 1$ for $I_{rel} > 1$ and $I_{rel} < 1$, respectively. Thus, the error in V_{rel} was corrected by adding 0.02 (V_{rel}) for $I_{rel} > 1$ and subtracting 0.015 (V_{rel}) for $I_{rel} < 1$.

Fluorescence spectroscopy

The effect of osmotic stress on the stability of split vaccine particles was examined by recording intrinsic fluorescence in the presence of osmotic gradients (0 and 0.3 osM) at pH 7.0/2.0 and 4 °C. Fluorescence was measured with split vaccine particles (200 μg/ml) at the excitation wavelength of 295 nm over the scanning range of 300–500 nm (slit size: 10 nm, scanning speed: 200 nm/min) using a fluorescence spectrophotometer (Cary Eclipse; Varian Inc., Palo Alto, CA, USA) (Choi et al. 2012a, 2013b, c). Split vaccine suspension in 300 mM sucrose (pH 7.0) and osmolyte sucrose solution (300 mM (iso-osmotic) and 900 mM (hyper-osmotic), pH 1.7) were mixed in an equal volume ratio to measure intrinsic fluorescence after incubation for 2 h at pH 2.0 and 4 °C. The acquired fluorescence spectra were corrected for background signal by measuring the same solution in the absence of vaccine. As a reference, fluorescence spectra were measured at iso-osmotic condition after mixing with 300 mM sucrose solution (pH 7.0) at 4 °C. After appropriate background correction, the peak shift and relative intensity change of emission maxima were examined with reference to the spectrum of vaccine in an iso-osmotic condition at pH 7.0.

HA activity of split vaccine at low pH

The effect of osmotic gradients (0 and 0.3 osM) on the functional HA activity of split vaccine at pH 2.0 and 4 °C was tested using hemagglutination assay as described previously (Hirst 1942; Choi et al. 2012b). HA activity of vaccine in iso-osmotic condition at 4 °C (pH 7.0) was taken as a reference and HA activity of samples at each condition was calculated relative to it.

Electron microscopy

The initial size and morphological change of influenza vaccine was analyzed using TEM (Philips/FEI CM20; FEI, Hillsboro, OR, USA). To prepare TEM samples, vaccine suspension was placed on a formvar-amorphous carbon-coated copper grid (Ted Pella, Redding, CA, USA). After removing excess solution by blotting with filter paper, samples were stained with 2 % phosphotungstic acid (pH = 7.0; Electron Microscopy Sciences, Hatfield, PA, USA) for 30 s. The samples were air-dried and stored in a desiccator before microscopic observation.

Statistical analysis

Minitab release 14 (Minitab, State College, PA, USA) was used for statistical analysis. Student's *t* test or analysis of variance (ANOVA; One-way, general linear model with Tukey's method) was used to analyze data. A *P* value of less than 0.05 indicated a significant difference.

Results and discussion

Figure 1 shows TEM micrographs of the prepared influenza vaccines in the form of (a) split virion and (b) WIV. The spherical structure in the image represents vaccine particles, identifiable by the presence of spike-like glycoproteins on the surface of the vaccine envelope. Split vaccine particles (Fig. 1a) maintained the same morphology as WIV vaccine particles (Fig. 1b), consistent with the previous report (Lee et al. 2011). However, it is interesting to note that split vaccine particles exhibited a statistically significant decrease in diameter compared to WIV vaccine particles (87 ± 17 nm for WIV vaccine and 30 ± 6 nm for split vaccine; *t* test, $P < 0.001$). Considering the fact that split vaccine is prepared by disintegration of WIV vaccine using Triton X-100, it is expected that reassembly of the disrupted WIV vaccine occurred upon removal of detergents during dialysis in a similar manner to liposomes (Ollivon et al. 2000). Furthermore, the observed hollow spherical structure of split vaccine particles makes them susceptible to size and shape changes caused by osmotic stress. Therefore, the osmotic behavior of split vaccine particles must be assessed to predict its stability in various gastric environments.

Short-term SFLS of influenza vaccine particles

SFLS analysis was performed by applying five different hyper-osmotic stresses ($\Delta = 0.025$, 0.05, 0.1, 0.15, and 0.3 osM), iso-osmotic stress ($\Delta = 0$ osM), and four different hypo-osmotic stresses ($\Delta = -0.05, -0.075, -0.1$, and -0.15 osM) to influenza vaccine particles at pH 2.0 and 4 °C (see Fig. 2a for split vaccine particles and 2b for WIV vaccine particles in hyper-, iso-, and hypo-osmotic conditions). It is noted that gastric contents/secretions

significantly influence the physiological gastric osmolarity (Hunt 1959, Choi et al. 2013b). Thus, vaccine particles can be subjected to hypo- (C_{ex} < 0.3 osM), iso- (C_{ex} = 0.3 osM), and hyper-osmotic pressures (C_{ex} > 0.3 osM) in the gastric environment. Therefore, in this work we used several representative osmotic pressures to investigate the time-dependent osmotic response of the vaccine particles using SFLS. Furthermore, because the effects of temperature on the SFLS behavior and stability of WIV vaccine were reported in our previous work (Choi et al. 2013b), SFLS analysis in this work was performed at 4 °C for vaccine samples to isolate the influence of osmotic stress in an acidic environment by eliminating the temperature effects.

Figure 2a shows SFLS curves observed for 8 s from split vaccine particles as a function of osmotic stress. The time course of I_{rel} exhibited a typical osmotic response. As shown in the plot 2a(i), SFLS spectra exhibited an increase in I_{rel} upon exposure to hyper-osmotic stress (≥0.05 osM) by the shrinkage of split vaccine particles. On the contrary, I_{rel} decreased with time due to the swelling in response to hypo-osmotic stress (2a(ii)). However, in both cases, I_{rel} saturation is reached at earlier stage with increasing osmotic stresses, indicating faster shrinkage or swelling in the presence of hyper- and hypo-osmotic stress, respectively. It is also noted that iso-osmotic stress (Δ = 0) showed a gradual decrease in scattering intensity (2a(ii)), which can be attributed to low pH-induced clustering of vaccine particles (Choi et al. 2013b). Such a decrease in I_{rel} is a general phenomenon when vaccine is incubated in acidic solution, regardless of osmotic stress. This explains the lack of intensity variation from split vaccine particles at Δ = 0.025 osM (see Fig. 2a-i).

Figure 2b shows the time course of I_{rel} at different osmotic gradients obtained from WIV vaccine particles. Osmotic responses of WIV vaccine particles were quite similar to those of split vaccine results shown in Fig. 2a. However, unlike the split vaccine particles, the SFLS spectra of WIV vaccine particles exposed to Δ = 0.025 osM generated a gradual intensity decrease, and no significant level of intensity variation was observed from hyper-osmotic gradients of 0.05 and 0.1 osM. This analysis implies the possibility that low pH-induced size increase of WIV vaccine is greater than that of split vaccine particles and/or split vaccine particles are more responsive to osmotic stress than WIV vaccine particles.

The rate constant (k) is plotted as a function of osmotic gradient (Δ) for split vaccine particles (Fig. 2c-i) and WIV vaccine particles (Fig. 2c-ii). As shown in Fig. 2c(i), k values of split vaccine were significantly higher upon exposure to hypo-osmotic stress (k = 2.2 ± 0.4/s, Δ = −0.15 osM) than hyper-osmotic stress (k = 0.5 ± 0.1/s, Δ = −0.15 osM). Both vaccine types showed an increase in k with increasing hypo-osmotic stress (ANOVA, P < 0.001). Based on the observations of the statistically higher k values (ANOVA, P < 0.001) of split vaccine particles than those of WIV vaccine particles at hypoosmotic stress, it was predicted that the resistance of virus wall to swelling was significantly lower in the split vaccine than in the WIV vaccine at the early stage of osmotic response. Furthermore, application of hyper-osmotic stress caused statistically significant differences in k values with vaccine type (ANOVA, P < 0.001), but this small variation between samples is of no practical significance.

Long-term SFLS of influenza vaccine particles

To characterize the long-term morphological changes of split vaccine particles in comparison with WIV vaccine particles, SFLS spectra were measured for 80 s after exposure to a hyper-osmotic gradient of 0.3 osM (pH 2.0, 4 °C). As previously observed with WIV vaccine particles at pH 2.0 and 37 °C (Choi et al. 2013b), the split vaccine particles also exhibited a step-wise intensity increase (Fig. 3a), i.e. the primary intensity increase at 0 s is followed by a secondary intensity increase at about 60 s. Assuming I_{rel} mainly depends on the size change of particles, split vaccine particles underwent a rapid volumetric shrinkage of <2 % during the first phase and showed progressive shrinkage after the onset time for the secondary shrinkage (t_{2nd}) until a steady-state is reached (t_{2nd}: ∼60 s, volumetric shrinkage: >25 %). In the case of WIV vaccine particles (pH 2.0, 4 °C) in Fig. 3b, a step-wise shrinking behavior was similarly observed in split vaccine (primary shrinkage: <9 %, secondary shrinkage: >40 %), but in a far more clear way.

The step-wise morphological change was predicted to be associated with the unique double-layered composite structure of the vaccine wall; a shell composed of a matrix protein (M1) array adheres to a lipid bilayer (Choi et al. 2013a). The generation of the secondary morphological change can be explained by the resistance of the M1 layer to further shrinkage, and importantly, t_{2nd} has been well correlated to the level of effective osmotic shock applied to vaccine particles (Choi et al. 2013a). Thus, although quantitative identification of protein components was not performed, the presence of the M1 layer in the wall of split vaccine particles supports the observation of the secondary shrinkage from SFLS spectra, thereby explaining the stepwise osmotic shrinkage in the same manner as WIV vaccine particles. Lower levels of volumetric shrinkage of split vaccine particles can be explained by its higher elastic compressibility modulus than that of WIV vaccine, due to smaller its diameter. It is known that elastic properties of liposomes are dependent on their size; a decrease in size has been reported to increase the elastic compressibility modulus (Sun et al. 1986). This probably caused the reduced hyper-osmotic shrinkage of split vaccine.

We next performed SFLS analysis at three different osmotic stresses ($\Delta = -0.15$, 0, and 0.15 osM) to identify the effects of the direction of the osmotic gradients on the long term swell-shrink characteristics of split vaccine (Fig. 4a). Time-courses of SFLS spectra of WIV vaccine particles were measured for comparison with split vaccine particles under the same test conditions (Fig. 4b). Upon exposure to hypo-osmotic stress, split vaccine exhibited a step-wise decrease in I_{rel} (Fig. 4a-i). As shown in Fig. 4a-ii, the initial and subsequent decrease in I_{rel} can be understood in terms of the step-wise volumetric change: vaccine swelled from 8 % at ∼135 s to 15 % at ∼157 s at $\Delta = -0.15$ osM. At hyper-osmotic stress or 0.15 osM, shrinkage also proceeded in a step-wise fashion, consistent with 80-s scan SFLS spectra. Since t_{2nd} is taken as an indicator of osmotic stress, the smaller t_{2nd} at 0.15 osM (Fig. 4a), compared to 0.3 osM (Fig 3a), can be explained by the lower osmotic stress (t test, $P < 0.001$). Also, a gradual decrease in I_{rel} at iso-osmotic stress can be attributed to a volume increase (<3 %) caused by low pH-induced vaccine aggregation (Choi et al. 2013b). While the observed change in osmotic stress-induced volumetric change of split vaccine was slightly less than that of WIV vaccine (compare Fig. 4a, b), it is thought that both vaccines

exhibit a similar osmotic swell-shrink behavior, due to their identical double-walled structure.

The effect of osmotic stress on t_{2nd} was measured by comparing SFLS curves obtained from both split vaccine and WIV vaccine at varying osmotic gradients (Fig. 4c). It is shown that t_{2nd} increases with decreasing magnitudes of osmotic stress. WIV vaccine exhibited significantly higher t_{2nd} relative to split vaccine (ANOVA, $P < 0.001$), but the most notable difference occurred at low osmotic stress, i.e. at $\Delta = -0.15$ and 0.15 osM. Therefore, the t_{2nd} data indicate that split vaccine would be more susceptible to osmotic stress-induced vaccine destabilization. The lower t_{2nd} of split vaccine compared with that of WIV vaccine implies the possibility of a decrease in mechanical strength via a detergent treatment. This is further supported by the well-known detergent-lipid/detergent-protein interactions, destabilizing lipid membranes during the solubilization process (le Maire et al. 2000). Hence, the change in the intrinsic mechanical properties of the split vaccine particle's wall probably resulted in a more rapid and enhanced osmotic response. On the contrary, it is possible that the intrinsically small size of split vaccine would limit its maximum level of volumetric change as discussed in Fig. 3. The interplay between detergent destabilizing effect and intrinsic size effect on mechanical property of the vaccine particles needs further study.

SFLS analysis was performed for 2 h to estimate the osmotic response of split vaccine during the gastric digestion. SFLS curves at a hyper-osmotic gradient of 0.3 osM were compared with those at iso-osmotic gradient. As expected, split vaccine exhibited shrinkage and pH-induced aggregation at hyper- and iso-osmotic stress, respectively (Fig. 5a for I_{rel} and 5b for V_{rel}). 2-h incubation in iso-osmotic, acidic solution resulted in a gradual decrease in I_{rel} (Fig. 5a) and thereby a progressive increase in V_{rel} to about 12 % (Fig. 5b). In the presence of hyper-osmotic stress, split vaccine shrank in a step-wise fashion consistent with shorter-term scans seen in Figs. 3a and 4a. It is important to note that SFLS spectrum displayed significant time-dependent intensity variations after reaching the secondary intensity saturation [see (ii) for a magnification of the selected area in (i)]. Unlike the WIV vaccine particles, which gradually decreased in intensity over time (Fig. S1), split vaccine particles showed no noticeable decrease in I_{rel} after 2 h of incubation. This indicates that osmotic pressure-induced defects in the split vaccine wall are rapidly reversed after allowing osmotic gradients to dissipate by diffusion of the osmolyte through the defect. Thus, two competing processes, the small defect generation and the recovery, seem to characterize hyper-osmotic shrinkage behavior of split vaccine particles, compared with the relatively large defects in WIV vaccine particles. As a result, it is reasonable to assume that the membrane perturbation may lead to destabilization of antigenic proteins and vaccine wall despite the difference in the undulation pattern of I_{rel}.

Effect of osmotic stress on the stability of influenza vaccine particles

Stability of the antigenic protein structure of split vaccine particles was evaluated by measuring intrinsic fluorescence and hemagglutination activity after incubation in iso- and hyper-osmotic conditions ($\Delta = 0$ and 0.3 osM, pH 2.0) for 2 h. The wavelength (Fig. 6a-i) and intensity (Fig. 6a-ii) of emission maximum were measured after exposure to acidic iso- and hyper-osmotic mediums and analyzed with the use of a reference (emission spectra

measured at Δ = 0 and pH 7.0). As shown in Fig. 6a, a significant level of red shift was observed after incubation in acidic iso-osmotic medium compared with controls, with further shift of emission spectra in acidic hyper-osmotic medium (One-way ANOVA, $P < 0.01$). The red shift indicates that the protein's aromatic amino acids are exposed to a more hydrophilic environment than those in neutral, iso-osmotic medium, a change likely due to pH and/or osmotic stress-induced conformational change (Teale and Weber 1957). This analysis is consistent with our previous study, showing that hyper-osmotic stress in acidic mediums had a significant destabilizing effect on WIV vaccine stability (Choi et al. 2013b). On the contrary, it is important to note that split vaccine showed an increase of relative intensity with increasing structural change, as shown in Fig. 6b (One-way ANOVA, $P < 0.001$). While we do not fully understand how emission intensity is regulated yet, opposite effects of antigen denaturation on fluorescence emission spectra have been previously observed for different strains (Luykx et al. 2004). To better characterize the vaccine-specific mechanisms, the relationship between vaccine type and fluorescence intensity needs further study.

TEM analysis was performed to observe the morphological change of split vaccine after incubation with acidic hyper-osmotic stress (Δ = 0.3 osM, pH 2.0) for 2 h. As shown in Fig. 6b, split vaccine lost its spherical shape and the spike-like glycoproteins covering the surface of the vaccine particle were no longer observed, indicating irreversible morphological change (compare Fig. 6b with Fig. 1a). This is consistent with our analyses of SFLS and intrinsic fluorescence.

To further support the combined deteriorative effects of low pH and hyper-osmotic stress on the functional activity of split vaccine, functional HA activity was assessed by measuring hemagglutination activity. As shown in Fig. 6c, 2-h incubation at Δ = 0.3 osM and pH 7.0 did not yield statistically significant HA activity difference compared with the control at Δ = 0 osM and pH 7.0 (t test, $P = 0.17$). In contrast, exposure to the acidic hyper-osmotic stress (Δ = 0.3 osM, pH 2.0) led to significant levels of HA activity loss. This can be explained by the membrane integrity loss of vaccine wall and conformational change of antigenic proteins, as demonstrated by SFLS, intrinsic fluorescence, and TEM. Therefore, it is clear that the hyper-osmotic stress-induced structural destabilization, as well as pH-induced antigen denaturation, contributed to the decrease in HA activity under acidic environments, consistent with our previous finding about WIV vaccine (Choi et al. 2013b). Since the stability and activity of HA proteins is critical in inducing broad immune response (Wiley and Skehel 1987; Staneková and Vareckova 2010; Quan et al. 2011; Choi et al. 2012b), it is likely that hyper-osmotic stress is a major factor in affecting the immunogenicity and efficacy of orally administered split influenza vaccine.

Conclusion

In the present study, we researched the destabilization of split vaccine in an acidic environment. The swell-shrink behavior of split vaccine particles was mainly investigated by analyzing SFLS spectra, and the results were compared with those obtained from WIV vaccine particles. We found that split vaccine displayed the same osmotic swelling/shrinking in response to hypo-/hyper-osmotic stress as WIV vaccine, which has been attributed to

identical hollow spherical morphology and composite wall structure. While split vaccine particles responded to osmotic stress more rapidly than WIV vaccine particles, its relative change in volume was less than that of WIV vaccine, probably due to the smaller particle size. Also, low pH-induced vaccine size increase was observed at acidic iso-osmotic medium. In particular, structural integrity of the split vaccine wall was lost upon exposure to hyper-osmotic stress, as indicated by an irregular light scattering pattern and TEM. As demonstrated by a red shift of intrinsic fluorescence spectra and by a significant level of HA activity loss, the membrane deformation resulted in further destabilization of the antigenic proteins than acid-induced conformational change alone. The results support that hyper-osmotic stress has a significant impact on the stability of the envelope-type split vaccine particles in an acidic environment, as has been found for WIV vaccines. Although osmotic stability was examined at 4 °C in this work, increased temperature, i.e. a physiological temperature (37 °C), accelerates the destabilization of influenza vaccine in acidic hyper-osmotic solution. We expect that increasing the viscosity of vaccine formulation, considering an inverse relationship between osmotic pressure and viscosity, as well as taking oral vaccine on an empty stomach may minimize osmotic stress-induced vaccine damage during digestion. Therefore, this research can be extended to study the stability of all envelope-type vaccines and thus, contribute to the development of stable oral vaccine formulations.

Supplementary Material

Refer to Web version on PubMed Central for supplementary material.

Acknowledgments

This study was conducted at the University of Alberta and the University of Cincinnati. Influenza vaccines used in this work were produced at the Georgia State University. This project was funded by a grant from the Bill & Melinda Gates Foundation through the Grand Challenges Exploration Initiative (C.D.M. and H.J.C.), and in part by NIH/NIAID grants AI093772 (S.M.K.), AI087782 (S.M.K.), and AI105170 (S.M.K). The funders had no role in study design, data collection and analysis, decision to publish, or preparation of the manuscript.

References

Azizi A, Kumar A, Diaz-Mitoma F, Mestecky J. Enhancing oral vaccine potency by targeting intestinal M cells. PLoS Pathogens. 2010; 6:e1001147. [PubMed: 21085599]

Bullough PA, Hughson FM, Skehel JJ, Wiley DC. Structure of influenza haemagglutinin at the pH of membrane fusion. Nature. 1994; 371:37–43. [PubMed: 8072525]

Choi HJ, Bondy BJ, Yoo DG, Compans RW, Kang SM, Prausnitz MR. Stability of whole inactivated influenza virus vaccine during coating onto metal microneedles. Journal of Controlled Release. 2013a; 166:159–171. [PubMed: 23246470]

Choi HJ, Ebersbacher CF, Kim MC, Kang SM, Montemagno CD. A mechanistic study on the destabilization of whole inactivated influenza virus vaccine in gastric environment. PLoS ONE. 2013b; 8:e66316. [PubMed: 23776657]

Choi HJ, Ebersbacher CF, Myung NV, Montemagno CD. Synthesis of nanoparticles with frog foam nest proteins. Journal of Nanoparticle Research. 2012a; 14:1–13. [PubMed: 22448125]

Choi HJ, Ebersbacher CF, Quan FS, Montemagno CD. pH stability and comparative evaluation of ranaspumin-2 foam for application in biochemical reactors. Nanotechnology. 2013c; 24:055603. [PubMed: 23324183]

Choi HJ, Yoo DG, Bondy BJ, Quan FS, Compans RW, Kang SM, Prausnitz MR. Stability of influenza vaccine coated onto microneedles. Biomaterials. 2012b; 33:3756–3769. [PubMed: 22361098]

Farag-Mahmod FI, Wyde PR, Rosborough JP, Six HR. Immunogenicity and efficacy of orally administered inactivated influenza virus vaccine in mice. Vaccine. 1988; 6:262–268. [PubMed: 3420975]

Fiore AE, Uyeki TM, Broder K, Finelli L, Euler GL, Singleton JA, Iskander JK, Wortley PM, Shay DK, Bresee JS, Cox NJ. Prevention and control of influenza with vaccines: recommendations of the Advisory Committee on Immunization Practices (ACIP), 2010. MMWR Recommendations and Reports. 2010; 59:1–62.

Giudice EL, Campbell JD. Needle-free vaccine delivery. Advanced Drug Delivery Reviews. 2006; 58:68–89. [PubMed: 16564111]

Harper SA, Fukuda K, Uyeki TM, Cox NJ, Bridges CB. Prevention and control of influenza: recommendations of the advisory committee on immunization practices (ACIP). MMWR Recommendations and Reports. 2004; 53:1–40.

Hirst GK. The quantitative determination of influenza virus and antibodies by means of red cell agglutination. Journal of Experimental Medicine. 1942; 75:49–64. [PubMed: 19871167]

Hunt JN. Gastric emptying and secretion in man. Physiological Reviews. 1959; 39:491–533. [PubMed: 13674903]

Lazzell V, Waldman RH, Rose C, Khakoo R, Jacknowitz A, Howard S. Immunization against influenza in humans using an oral enteric-coated killed virus-vaccine. Journal of Biological Standardization. 1984; 12:315–321. [PubMed: 6480615]

Le Maire M, Champeil P, Moller JV. Interaction of membrane proteins and lipids with solubilizing detergents. Biochimica et Biophysica Acta. 2000; 1508:86–111. [PubMed: 11090820]

Lee IS, Kim HJ, Lee DH, Hwang GB, Jung JH, Lee M, Lim J, Lee BU. Aerosol particle size distribution and genetic characteristics of aerosolized influenza A H1N1 virus vaccine particles. Aerosol Air Qual Res. 2011; 11:230–237.

Luykx DM, Casteleijn MG, Jiskoot W, Westdijk J, Jongen PM. Physicochemical studies on the stability of influenza haemagglutinin in vaccine bulk material. European Journal of Pharmaceutical Sciences. 2004; 23:65–75. [PubMed: 15324924]

Mutsch M, Zhou W, Rhodes P, Bopp M, Chen RT, Linder T, Spyr C, Steffen R. Use of the inactivated intranasal influenza vaccine and the risk of Bell's palsy in Switzerland. New England Journal of Medicine. 2004; 350:896–903. [PubMed: 14985487]

Neutra MR, Kozlowski PA. Mucosal vaccines: the promise and the challenge. Nature Reviews Immunology. 2006; 6:148–158.

Ollivon M, Lesieur S, Grabielle-Madelmont C, Paternostre M. Vesicle reconstitution from lipid-detergent mixed micelles. Biochimica et Biophysica Acta. 2000; 1508:34–50. [PubMed: 11090817]

Palese P. Making better influenza virus vaccines? Emerging Infectious Diseases. 2006; 12:61–65. [PubMed: 16494719]

Quan FS, Compans RW, Nguyen HH, Kang SM. Induction of heterosubtypic immunity to influenza virus by intranasal immunization. Journal of Virology. 2008; 82:1350–1359. [PubMed: 18032492]

Quan FS, Li ZN, Kim MC, Yang D, Compans RW, Steinhauer DA, Kang SM. Immunogenicity of low-pH treated whole viral influenza vaccine. Virology. 2011; 417:196–202. [PubMed: 21722934]

Skehel JJ, Bayley PM, Brown EB, Martin SR, Waterfield MD, White JM, Wilson IA, Wiley DC. Changes in the conformation of influenza-virus hemagglutinin at the pH optimum of virus-mediated membrane-fusion. Proceedings of the National Academy of Sciences USA. 1982; 79:968–972.

Staneková Z, Vareckova E. Conserved epitopes of influenza A virus inducing protective immunity and their prospects for universal vaccine development. Virology Journal. 2010; 7:351. [PubMed: 21118546]

Sun ST, Milon A, Tanaka T, Ourisson G, Nakatani Y. Osmotic swelling of unilamellar vesicles by the stopped-flow light-scattering method-elastic properties of vesicles. Biochimica et Biophysica Acta. 1986; 860:525–530.

Szarka LA, Camilleri M. Methods for measurement of gastric motility. American Journal of Physiology Gastrointestinal and Liver Physiology. 2009; 296:G461–G475. [PubMed: 19147807]

Teale FW, Weber G. Ultraviolet fluorescence of the aromatic amino acids. Biochemical Journal. 1957; 65:476–482. [PubMed: 13412650]

Thompson WW, Shay DK, Weintraub E, Brammer L, Cox N, Anderson LJ, Fukuda K. Mortality associated with influenza and respiratory syncytial virus in the United States. JAMA. 2003; 289:179–186. [PubMed: 12517228]

Wiley DC, Skehel JJ. The structure and function of the hemagglutinin membrane glycoprotein of influenza virus. Annual Review of Biochemistry. 1987; 56:365–394.

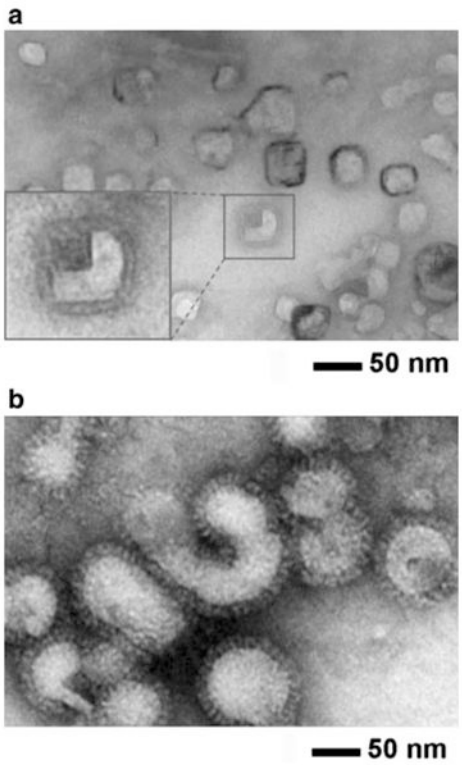

Fig. 1.

Negative-stain TEM micrographs of influenza vaccine particles. Inactivated A/PR/8/34 (H1N1) influenza virus vaccines. **a** split vaccine particles and **b** whole inactivated virus (WIV) vaccine particles. Vaccines incubated in iso-osmotic sucrose medium (pH 7.0, 4 °C) were stained with phosphotungstic acid (2 %, pH 7.0) and allowed to dry under ambient conditions before imaging. *Inset* at the *left bottom* in **a** shows magnified split vaccine image. Vaccine particle size was determined by TEM image analysis for split vaccine particles (30 ± 6 nm in diameter, $n = 30$) and WIV vaccine particles (87 ± 17 nm in diameter, $n = 80$)

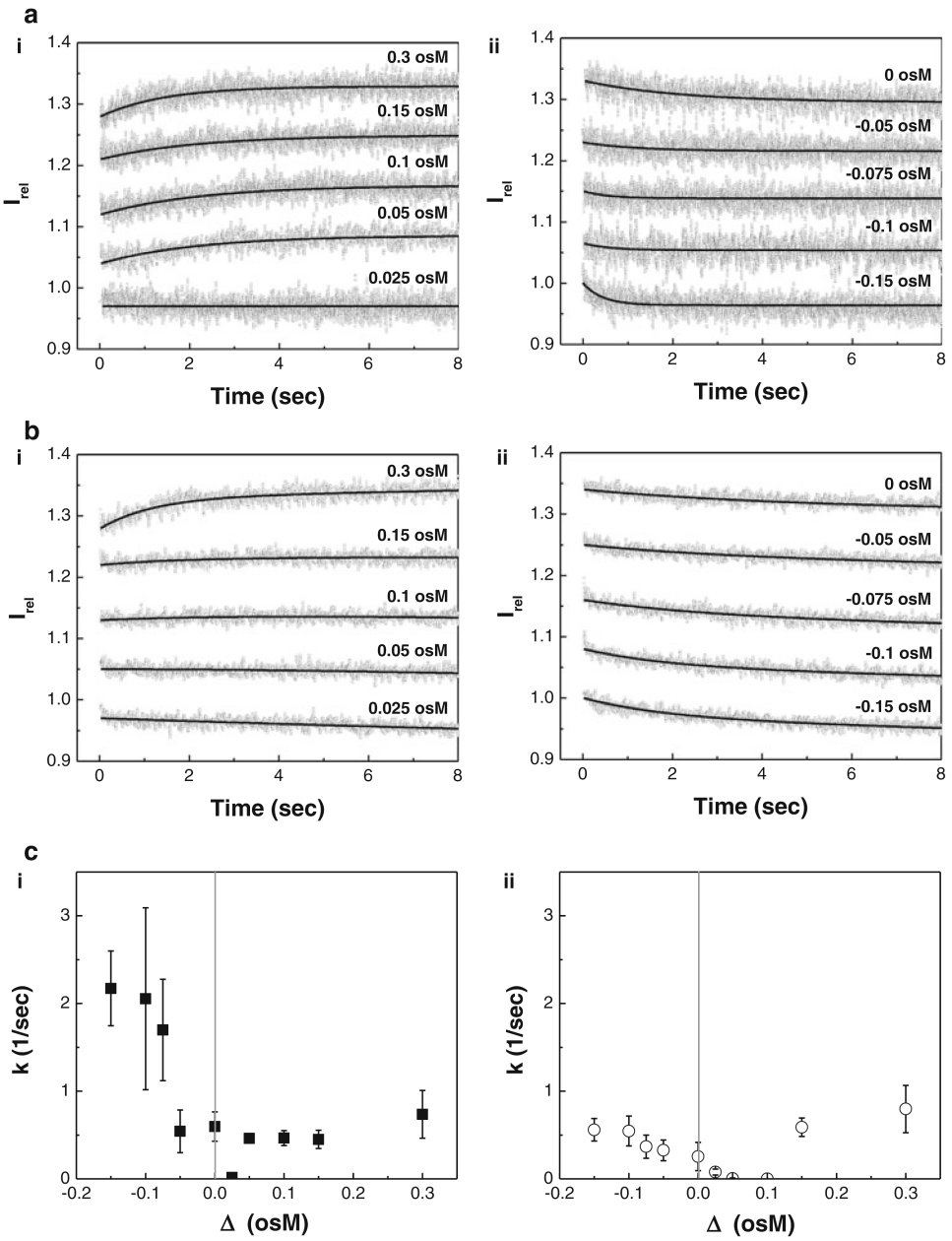

Fig. 2.

A comparison of osmotic swelling/shrinking behavior of influenza vaccine particles at pH 2.0. 8-s scan SFLS spectra of the split **a** and WIV **b** vaccine particles subjected to (*i*) hyper and (*ii*) iso-/hypo-osmotic shocks using sucrose at 4 °C and c their corresponding rate constant (*k*) as a function of osmotic gradients ($\Delta = C_{ex} - C_{in}$, i.e. the difference in osmolarity between the external and inner medium) for (*i*) split and (*ii*) WIV vaccine particles. The osmotic behavior of the vaccine particles was investigated by recording scattered light intensity (I) at 546 nm upon exposure to ten different concentrations of acidic sucrose solutions (hyper-, iso-, and hypo-osmotic stress) at pH 2.0. The relative light scattering data ($I_{rel} = I/I_0$, I_0: initial intensity at time zero, I: intensity at time t) are

represented in (**a**, **b**) and the solid curve is a fit to the I_{rel} data points. I_{rel} of SFLS spectra in (**a**, **b**) are offset for clarity, but the intensity scale is same for all spectra. Spectra are representative of n = 30–170 replicates at each condition. I_{rel} and k corresponding to WIV vaccine at 0.3 osM (pH 2.0, 4 °C) shown in **b**(*i*) and *c*(*ii*) are reused from an earlier report (Choi et al. 2013b)

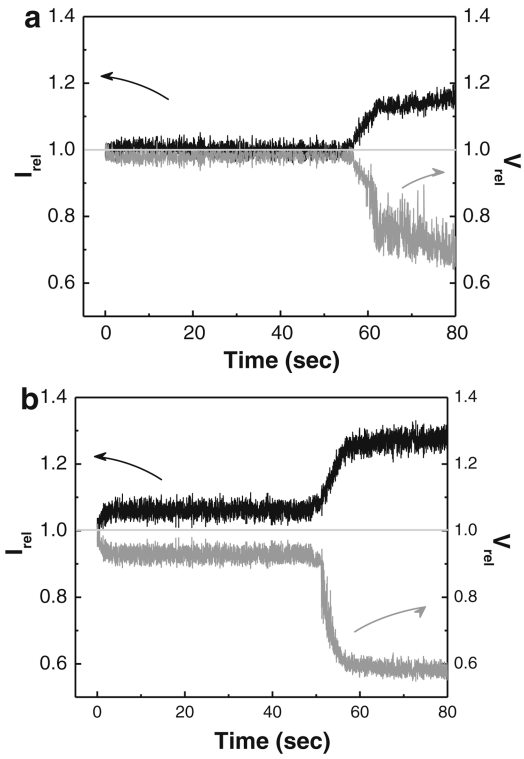

Fig. 3.

Step-wise morphological change of influenza vaccine particles. The osmotic shrinkage behavior of the particles (**a** split vaccine, **b** WIV vaccine) was comparatively investigated by applying a hyper-osmotic gradient of 0.3 osmolarity (osM) at pH 2.0 and 4 °C. The relative volume ($V_{rel} = V/V_{iso}$, V_{iso}: volume in iso-osmotic solution, volume at time t) was calculated from the $I_{rel} - V_{rel}$ relationship previously established for PC-liposome model. Spectra are representative of $n = 6$ and ten replicates for WIV vaccine and split vaccine, respectively, examined at each condition

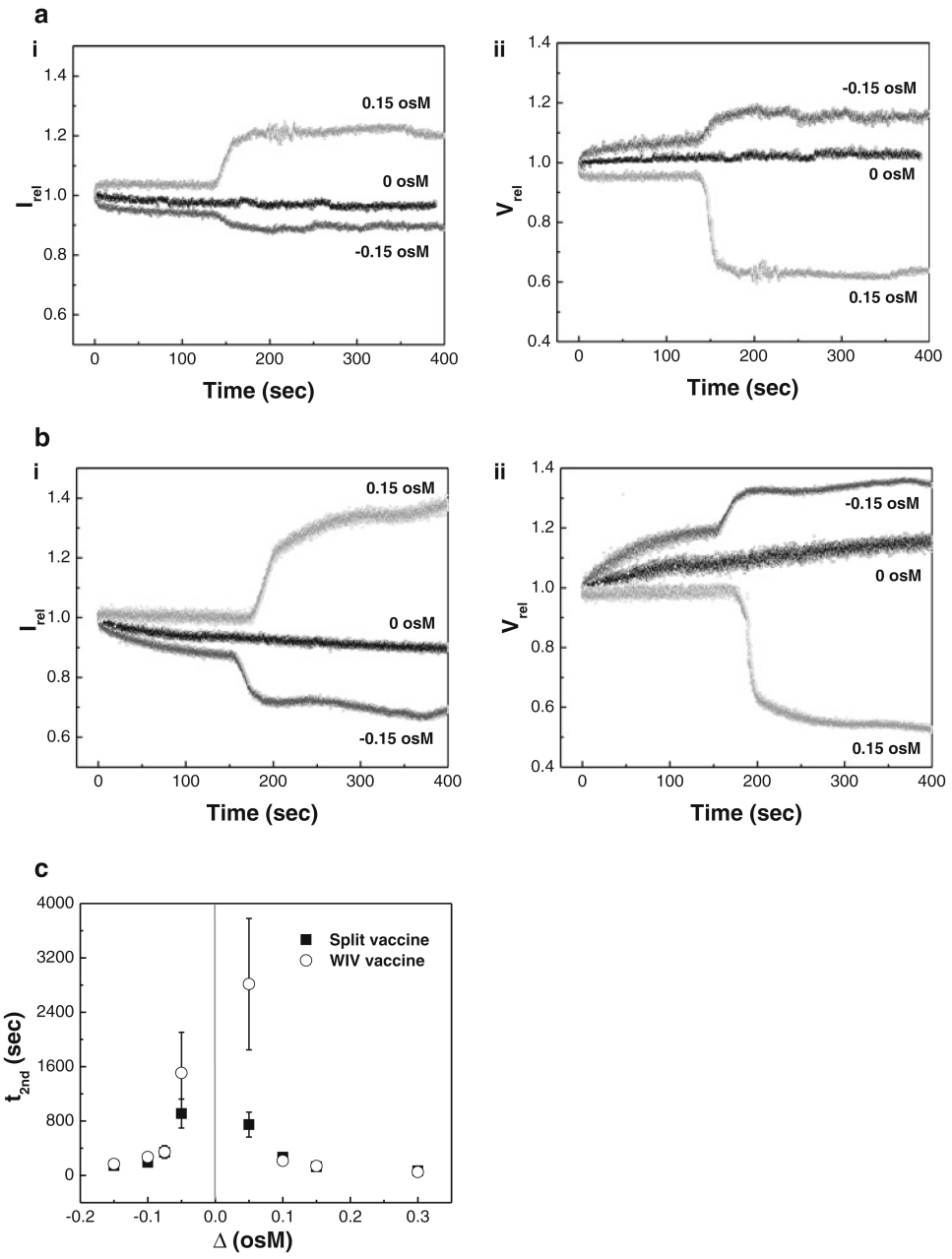

Fig. 4.

The effects of osmotic stress on the time-dependent osmotic response of influenza vaccine particles. (*i*) I_{rel} of SFLS curves and (*ii*) V_{rel} of influenza vaccine particles (**a** split vaccine particles, **b** WIV vaccine particles) corresponding to I_{rel} in part (*i*) in response to hypo-, iso-, and hyper-osmotic stress (Δ = −0.15, 0, and 0.15 osM). **c** Onset time for the secondary shrinkage (t_{2nd}) as a function of osmotic gradient at pH 2.0 (*filled square* split vaccine particles, *empty circle* WIV vaccine particles). (Mean ± SD; *n* = 3–15.) The t_{2nd} data corresponding to WIV vaccine particles at 0.3 osM (pH 2.0, 4 °C) were reused from an earlier report (Choi et al. 2013b)

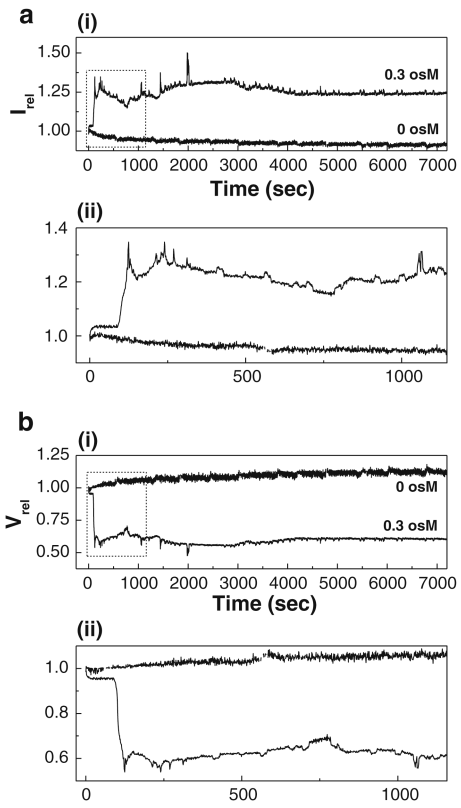

Fig. 5.

Long-term course of morphological change of split vaccine particles. **a** Long-term course of SFLS curves (I_{rel}) and **b** V_{rel} of influenza split vaccine particles exposed to iso- and hyper-osmotic gradient (0 and 0.3 osM) at pH 2.0 and 4 °C for 2 h. Magnified SFLS spectra and V_{rel} corresponding to the selected area in (*i*) are shown in (*ii*). Spectra are representative of *n* = 6 replicate samples

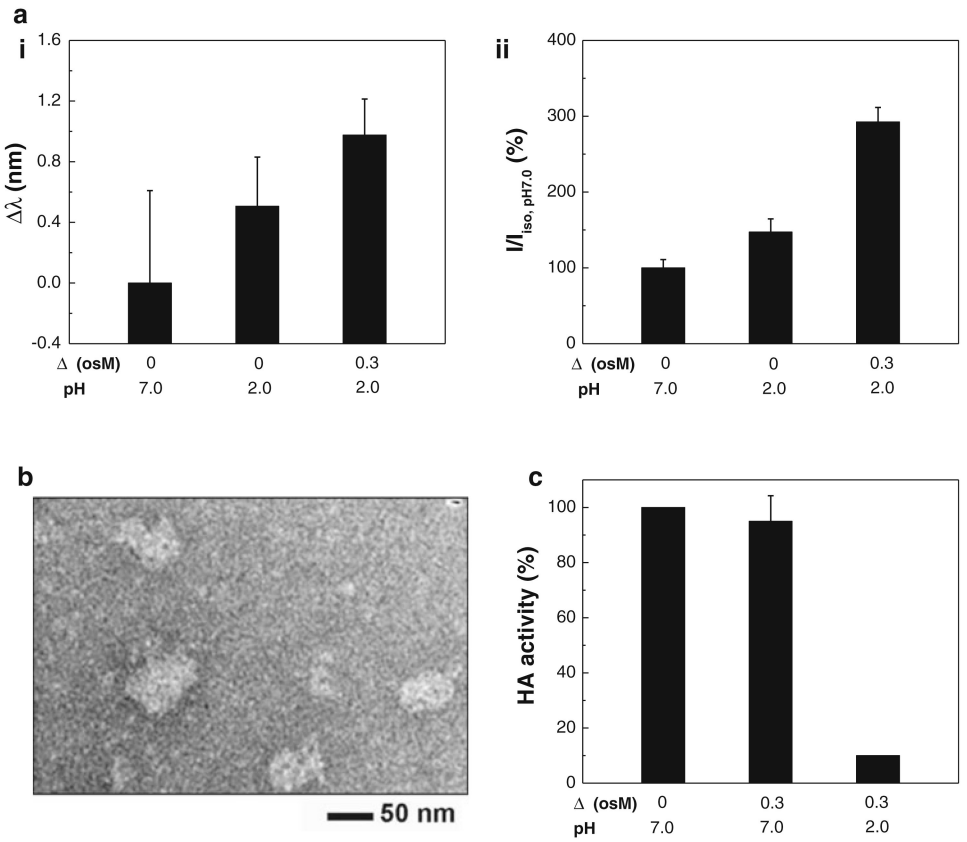

Fig. 6.

Structural stability of split vaccine. **a** Intrinsic fluorescence spectra of split vaccine particles: (*i*) shifts in maximum emission wavelength ($\Delta\lambda = \lambda - \lambda_{iso\ pH\ 7.0}$), (*ii*) relative intensity of emission maxima ($I/I_{iso,\ pH\ 7.0}$). The maximum emission position and intensity relative to control (pH 7.0) were analyzed from fluorescence spectra measured from split vaccine particles after 2 h of incubation at 4 °C. (Mean ± SD; *n* = 6.). **b** TEM micrograph of split vaccine particles incubated in acidic hyper-osmotic medium (Δ = 0.3 osM, pH 2.0) for 2 h. c HA activity of split vaccine particles. Hemagglutinating activity of split vaccine in acidic hyper-osmotic medium was measured after 2 h of incubation, and the functional HA activity relative to control (Δ = 0 osM, pH 7.0) is shown for comparison (Mean ± SD; *n* = 8)